Catal Lett
DOI 10.1007/s10562-015-1525-4

Facile Ester Synthesis on Ag-Modified Nanoporous Au: Oxidative Coupling of Ethanol and 1-Butanol Under UHV Conditions

Kara J. Stowers[1] · **Robert J. Madix**[2] · **Monika M. Biener**[3] · **Juergen Biener**[3] · **Cynthia M. Friend**[4]

Received: 15 February 2015 / Accepted: 31 March 2015

Abstract A dilute Ag alloy of nanoporous Au (npAu) has been shown to self-couple methanol with 100 % selectivity and high conversion under catalytic flow conditions. However, because prior studies in flow reactors showed difficulty in self-coupling ethanol and 1-butanol over npAu in flow reactors, the inherent capability on npAu for self-coupling of ethanol and 1-butanol was examined under ultrahigh vacuum conditions on identical npAu catalysts. This study shows that the oxygen-covered Ag-modified npAu does efficiently effect the self-coupling of ethanol and 1-butanol under UHV conditions. The coupling is initiated by adsorbed atomic oxygen formed from O_2 dissociation via a chemisorbed molecular state. The amount of ester formed increases with the degree of oxygen precoverage at the expense of aldehyde production. Repeated annealing of the catalyst above 550 K for temperature programmed reaction changes the ligament and pore sizes, affecting the product distribution, but high reactivity is sustained over many heating cycles.

Graphical Abstract

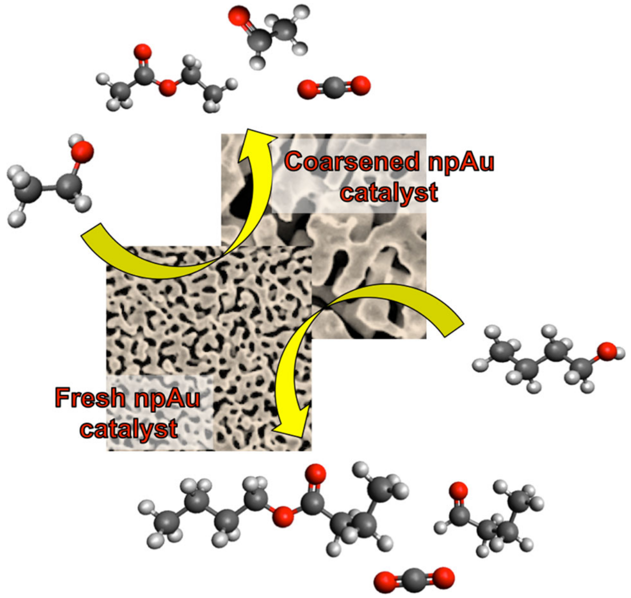

Keywords Nanoporous gold · Selective oxidation · Ethanol · 1-Butanol · Ester formation · Aerobic oxidation · Catalysis

1 Introduction

Nanoporous gold (or, more precisely, in this case a dilute nanoporous alloy of silver in gold) is an unsupported catalyst material which has been shown to catalyze the selective oxidation of CO and the oxygen-assisted self-coupling of methanol effectively under steady state conditions at atmospheric pressure [1–3]. However, the self-coupling of ethanol and 1-butanol was observed to be much

---

Electronic supplementary material The online version of this article (doi:10.1007/s10562-015-1525-4) contains supplementary material, which is available to authorized users.

✉ Cynthia M. Friend
friend@fas.harvard.edu

[1] Chemistry and Biochemistry, Brigham Young University, Provo, USA

[2] School of Engineering and Applied Sciences, Harvard University, Cambridge, USA

[3] Lawrence Livermore National Laboratory, Livermore, USA

[4] Harvard University, Cambridge, USA

less efficient in subsequent reactor studies, despite the fact that these reactions occur as readily as methanol self-coupling in model studies on oxygen precovered single crystal surfaces of gold [4, 5]. Moreover, in the previously reported studies of the partial oxidation of ethanol and 1-butanol on npAu, aldehyde formation was predominant [4], unlike the result for the oxygen-assisted self-coupling of methanol, for which methyl formate was formed with nearly 100 % selectivity [6]. Because npAu is a freestanding metallic material, it is amenable to model studies using the tools of ultrahigh vacuum. We have thus examined these coupling reactions on npAu in UHV in order to ascertain if there are inherent limitations to the coupling reactions of higher alcohols on npAu and to guide our thinking about this class of catalytic reactions on npAu.

2 Experimental

All experiments were conducted in an ultrahigh vacuum chamber (with a base pressure below 4×10^{-10} torr) using the same nanoporous gold catalyst materials used in flow reactor experiments already reported [4, 6]. Catalysts were obtained from Lawrence Livermore National Laboratory and prepared following previously published procedures for dealloying [7] to obtain an unsupported nanoporous gold catalyst with 30–50 nm sized ligaments and pores and 1–3 at.% bulk Ag (Fig. S1, Supporting Information). Further characterization of the elemental composition was conducted with ex situ X-ray photoelectron spectroscopy. The active catalyst surface was prepared in situ by iterative exposure of npAu to ozone which effectively removes any residual carbon [8, 9]. The O_2 exposure that yielded saturation coverage was determined by exposing the surface to increasing doses of oxygen until the integrated area of the oxygen recombination temperature programmed desorption peak leveled off (Fig. S2, Supporting Information).

For the reaction studies, the pre-conditioned npAu catalyst was exposed to molecular oxygen at 300 K by backfilling the vacuum chamber via a leak valve, and all exposures reported here are in units of Langmuir ($1\ L = 10^{-6}$ Torr s). The relative oxygen coverage (in percent of the saturation coverage) was determined by comparison with the oxygen saturation calibration curve (see below). Ethanol and 1-butanol were introduced to the catalyst surface at the temperatures specified (typically below 180 K) by monitoring the ambient pressure in the chamber. Surface concentrations of O_{ads} used were relatively low (10 % of saturation) in order to minimize over oxidation of the alcohols [10]. It is not possible to determine the absolute coverage of O_{ads} on npAu because the active surface area was not known. A typical experiment consisted of oxygen exposure to the catalyst surface at 300 K followed by cooling of the sample to 180–140 K before dosing the alcohol. A trace amount of water condensed on the surface during cooling (less than 1 % of the amount observed in a typical alcohol oxidation reaction). The catalyst was then heated, and the reaction monitored by temperature programmed reaction spectroscopy (TPRS) according to well-established protocols [11]. The heating rate for all temperature programmed reactions was nearly constant at $\sim 3 \pm 0.5\ K\ s^{-1}$. The reaction products were identified by quantitative mass spectrometry (Hiden HAL/3F) using fragmentation patterns obtained from authentic samples (see Supporting Information).

3 Results

3.1 Oxygen Activation and Calibration on npAu

Three distinct desorption peaks were observed for O_2 in temperature-programmed desorption following exposure of the npAu to O_2 at 130 K (Fig. 1). The dominant peaks emerge at 270 and ~550 K for intermediate doses (30–90 L), increasing in magnitude with increasing exposure. The peak temperatures of the two low temperature features remain constant with increasing O_2 coverage, whereas the peak temperatures of the high temperature species shift to

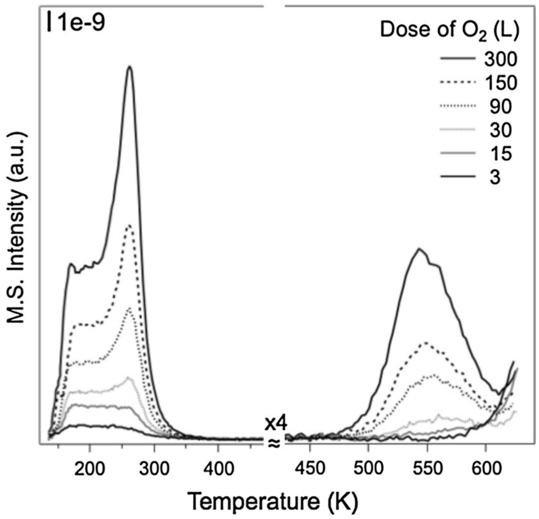

Fig. 1 Evolution of adsorbed molecular and atomic states of oxygen following dosing of the npAu surface with oxygen in UHV. Dioxygen dosed from 3 to 300 Langmuir at 130 K shows molecular desorption at 170 and 270 K and atomic recombination near 550 K. A nearly linear heating rate of $3\ K\ s^{-1}$ was used. The sample was prepared by cleaning at 300 K in UHV with a direct dose of an ozone-rich oxygen followed by 130 annealing cycles up to 600 K observing methanol oxidation

lower temperatures with increasing coverage (doses of 30 L–300 L respectively). Adsorption of an isotopic mixture of O_2 was used to demonstrate that the two lower temperature peaks are due to reversible adsorption of molecular O_2, whereas the peak near 550 K is due to recombination of adsorbed atomic O (Fig. S3). Following adsorption of a mixture of $^{16}O_2$ and $^{18}O_2$, only $^{16}O_2$ and $^{18}O_2$ were detected below 350 K, whereas $^{16}O_2$, $^{18}O^{16}O$, and $^{18}O_2$ were evolved simultaneously from 450 to 600 K. The rise in intensity above 600 K is attributed to subsurface oxygen in analogy to prior work [12]. The observed oxygen desorption behaviour is analogous to that observed for single crystal silver surfaces [13, 14]. The temperature of desorption of the molecular state, however, is approximately 100 K higher than from either Ag(110) or Ag(111) [13, 14]. However, the temperature at which the adatoms recombine is lower than on Ag(110) and characteristic of mixed Ag–Au sites on an Ag/Au alloy surface [15], indicating a pronounced effect of metal alloying on the reactivity of the npAu. The data strongly suggest that adsorbed atomic oxygen is formed via dissociation of a chemisorbed molecular oxygen state associated with silver or modified silver sites at the surface. In contrast to bulk gold, which neither chemisorbs nor activates dioxygen, the nanoporous gold catalyst chemisorbs dioxygen and activates it at relatively low temperature. Consequently, exposure of the npAu to dioxygen at 300 K yields only adsorbed atomic oxygen.

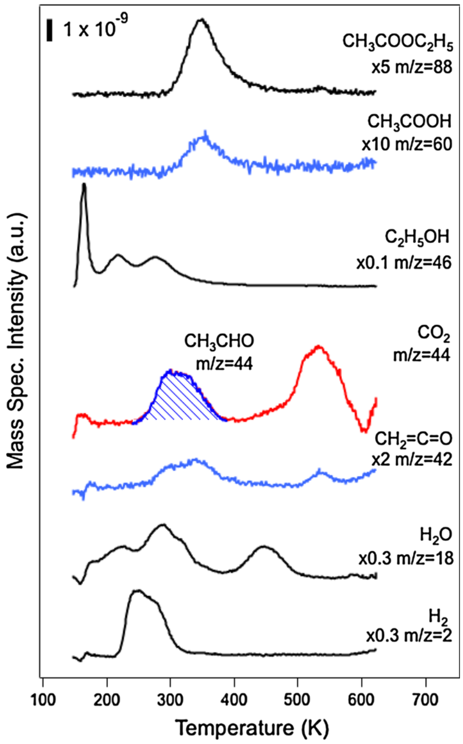

Fig. 2 Temperature programmed reaction of ethanol on npAu. 60 Langmuir of dioxygen was dosed at 300 K to achieve 10 % saturation coverage. Subsequently, 1.5 L ethanol was dosed at 140 K. Overlapping mass fragments have been subtracted for clarity. The m/z = 44 mass indicates acetaldehyde evolution at 300 K (*shaded*) and CO_2 evolution at 550 K. The heating rate was 3 K s^{-1}

3.2 Oxygen Mediated Coupling of Ethanol on npAu

Ethanol reacts readily with O/npAu ($\sim$10 % saturation), mainly forming ethyl acetate and acetaldehyde during temperature programmed reaction (Fig. 2). Ethyl acetate accounts for 48 % of the products and acetaldehyde for 29 %. Approximately 17 % of the product is CO_2. The remaining C-containing products are acetic acid (2 %) and ketene (4 %). Both H_2 and water are also detected and are produced from O–H and C–H bond scission.

There is clear evidence of bond activation at low temperature based on the fact that water and dihydrogen evolution begins below room temperature. Water is evolved in several discernable peaks at 190, 220, 290, 310 and 450 K (Fig. 2). Acetaldehyde is formed in a broad peak which may consist of two components, with an onset of 260 K; the maximum rate of acetaldehyde is at 290 K, coincident with one of the water peaks (Fig. 2). Ethyl acetate and acetic acid are evolved at 350 K (Fig. 2).

Combustion to H_2O and CO_2 occur at higher temperature with water peaks at 450 K and CO_2 at 550 K (Fig. 2). The CO_2 is accompanied by a small amount (each less than <1 %) of various other products that are characteristic of the decomposition of adsorbed acetate on Au(111) [16], including ethyl acetate, ketene, and water. There was no oxygen recombination at 550 K demonstrating that all adsorbed O was reacted away. Overall, the reaction pattern is similar to that observed from exposure of O/Au(111) to ethanol.

3.3 Oxygen Mediated Coupling of 1-Butanol on npAu

1-Butanol is also selectively oxidized on the npAu following adsorption of O, forming butyl butyrate (40 %) and butyraldehyde (23 %) as the major products (Fig. 3). Carbon dioxide is a more substantial product for 1-butanol *vs* ethanol, accounting for 37 % of the products even at the relatively low surface O concentration of $\sim$10 %. Both butyl butyrate and butyraldehyde also form from reaction of 1-butanol on O/Au(111). Both H_2O and H_2 form at very low temperature, as observed for ethanol. Water is produced in a well-defined peak at 260 K, which coincides with a 1-butanol peak and with the production of butyraldehyde. There is an H_2 peak at 210 K with a shoulder at 260 K.

The onset of butyraldehyde production is $\sim$300 K; water and 1-butanol are concomitantly evolved and there is

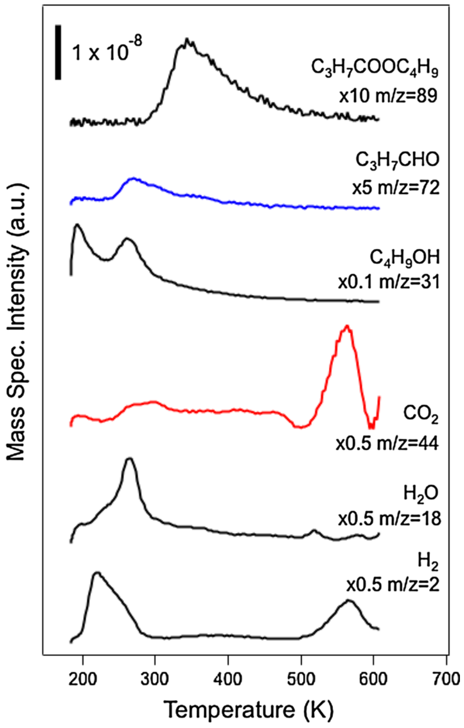

Fig. 3 Temperature programmed reaction of 1-butanol on npAu. 30 Langmuir of dioxygen was dosed at 300 K to achieve 10 % saturation coverage. Subsequently, 1.0 Langmuir of 1-butanol was dosed at 180 K. Overlapping mass fragments have been subtracted for clarity. The heating rate was approximately 3 K s^{-1}

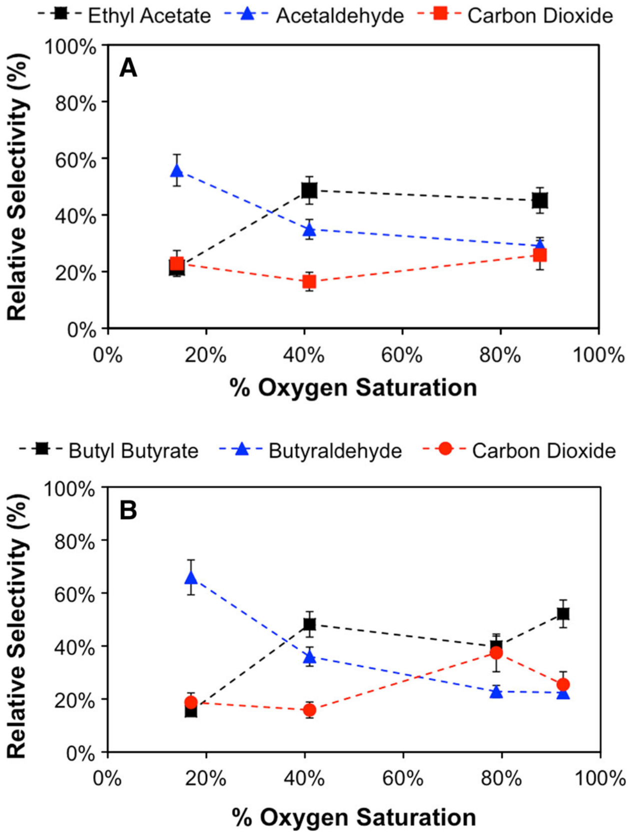

Fig. 4 **a** Selectivity dependence on oxygen coverage for ethanol oxidation. Dioxygen was dosed at 300 K from 15 to 300 Langmuir to obtain 20–95 % saturation coverage. **b** Selectivity dependence on O_2 for 1-butanol oxidation. Dioxygen was dosed at 300 K from 1.5 to 15 Langmuir. Conversion and selectivity were obtained from TPRS data at each O_2 coverage. *Lines* are drawn to direct the eye only

a shoulder on the hydrogen peak. There is only a small amount of water in the temperature range where butyl butyrate is formed. In addition, H_2 and CO_2 are produced near 560 K (Fig. 3).

3.4 Effect of Oxygen Coverage on Alcohol Oxidation

Except at the lowest initial oxygen coverages, the reaction selectivities for both ethanol and 1-butanol are only weakly dependent on the surface concentration of preadsorbed O (Fig. 4). Below 40 % saturation coverage by oxygen, the respective aldehydes are the main products, whereas above 40 % self-coupled products dominate. The amount of CO_2 is relatively independent of oxygen coverage. These results are also consistent with the product distributions seen on single-crystal gold in ultrahigh vacuum studies [5, 17]. The trends were reproducible for different samples of npAu.

3.5 General Mechanistic Features

Though the purpose of this paper is to demonstrate the inherent capability of npAu to self-couple ethanol and 1-butanol, it is appropriate to comment briefly on the general mechanistic features of the reactions observed here. First, the concurrent evolution of aldehyde, hydrogen, water, and the parent alcohol (Figs. 2, 3) is typical of β-H elimination from the adsorbed alkoxy species from the preoxidized surface, the key reactive intermediate identified for these reactions on model gold single crystals [9, 18]. It is well known that the aldehyde is formed from reaction of the alcohol with preadsorbed oxygen [18]. Following the aldehyde formation the ester is formed via reaction of the adsorbed aldehyde with remaining adsorbed alkoxy. As hydrogen evolution is atypical of these reactions on pure gold but is seen on metallic Ag, it appears that silver may make an independent contribution to the overall chemistry of the reactions on the npAu alloy catalysts studied here. However, it is important to note that these self-coupling reactions do not occur on pure silver surfaces and must be attributed to reactions on the gold or silver-gold alloy sites. These details are currently under further investigation. The general conclusion is that npAu does inherently and effectively promote the self-coupling of higher molecular weight alcohols.

3.6 Evolution of Morphology of npAu

Nanoporous gold, as prepared by free corrosion in concentrated nitric acid, has pores and ligaments that range from 30 to 50 nm in diameter, which was confirmed here using scanning electron microscopy (SEM) [19]. Energy dispersive X-ray spectroscopy (EDX) was used to determine the elemental composition of the catalyst. The structure of the catalyst is unchanged at temperatures lower than 425 K when treated with ozone in a flow reactor [20], however after successive temperature programmed reactions involving annealing above 450 K the structure begins to coarsen (Fig. 5). The temperature programmed experiments performed here required annealing from low temperatures up to 600 K at 3–6 K s^{-1} and therefore the catalyst spends ~1 min per cycle above 450 K. Over time the ligament and pore sizes increased from 40 and 50 nm to 190 and 150 nm, and the estimated surface area also decreases from 4.7 to 1.0 m^2 g^{-1} accordingly [21]. The total silver content in samples as measured by EDS ex situ is 2.4 ± 0.5 % silver for both fresh and coarsened samples. This decrease in surface area and change in morphology, however, did not significantly affect the overall reactivity of the npAu for the self-coupling of ethanol, though changes in selectivity were observed (Fig. 6); comparable studies for 1-butanol were not performed. The thermal stability of the npAu under steady-state conditions is currently being investigated.

4 Discussion

Adsorbed atomic oxygen, readily generated by dissociation of chemisorbed dioxygen on npAu, is the form of surface oxygen responsible for the oxygen-assisted self-coupling reactions observed on the npAu in this study. The chemisorbed state of dioxygen must originate from binding that involves surface silver atoms [22, 23], but it exhibits different reactivity. The lowest temperature molecular state peak observed on the npAu desorbs at 170 K, as does the chemisorbed dioxygen state on Ag(110) [14, 24, 25]. On Ag(110), upon heating, desorption of chemisorbed molecular oxygen competes with its dissociation between 130 and 170 K. The primary peak for molecular O_2 desorption from npAu is, however, significantly higher in temperature than observed on either Ag(110) or Ag(111) [13, 14, 26, 27]. On the other hand, the temperature for oxygen *recombination* on npAu is similar to that expected on gold (540 K), occurring at a lower temperature than observed on silver surfaces (580 K) [14, 28, 29]. These results suggest that dioxygen is chemisorbed on silver sites on the surface that are modified by surrounding gold atoms, but that atom recombination occurs predominantly from the surrounding gold surface. The low silver content (2.5 %) in the catalyst facilitates activation of dioxygen, and the npAu exhibits the reactivity and selectivity for oxygen-assisted coupling of the alcohols that is characteristic of metallic gold [9].

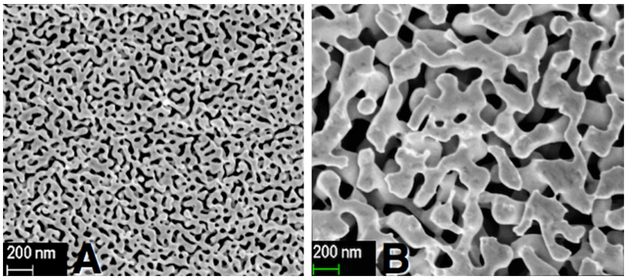

Property	Sample A	Sample B
Ave. Pore Size (nm)	50	150
Ave. Ligament Size (nm)	40	192
Ag by EDS (%)	2.6	2.3

Fig. 5 Scanning electron micrograph (SEM) images of the npAu catalyst before reactions in ultrahigh vacuum (**a**) and after (**b**) ozone treatment and reactions. The ligament structure has increased from ~50 nm in pore and ligament size to ~160 nm while retaining activity for oxidative coupling

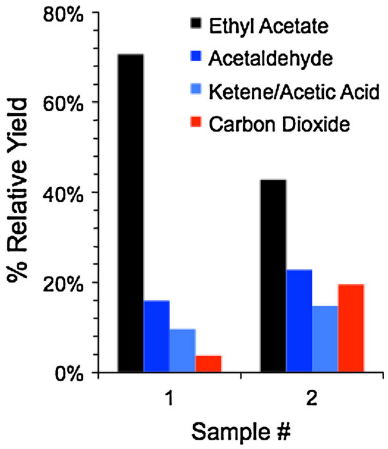

Fig. 6 Product distributions of a nanoporous gold catalyst before (*1*) and after (*2*) 65 different reactions with annealing to 600 K. Initial oxygen coverages were approximately 20 % of surface oxygen saturation

The primary purpose of this study was to apply the well defined conditions of ultrahigh vacuum to O-covered npAu to determine its capability to self-couple longer chain alcohols (ethanol and 1-butanol) to form their respective esters (ethyl acetate and butyl butyrate), as is observed on O/Au(111). In fact, we demonstrate here that oxygen-activated npAu facilely promotes self-coupling of both of the longer-chain alcohols, ethanol and 1-butanol, yielding their corresponding esters as the primary products. The extent of coupling reported here is significantly larger than reported in the previous studies under catalytic conditions [4, 6]. Low initial oxygen coverage appears to favor aldehyde

Table 1 Temperatures for β-C–H scission of adsorbed alkoxy on the surface

Surface	Adsorbed RO	Temperature for β C-H scission (K)
npAu	CH_3CH_2O	300
Ag(110)	CH_3CH_2O	275
Au(111)	CH_3CH_2O	<235
$Ag_{0.4}/Au_{0.6}(111)$	CH_3O	<260

production, while higher (although not excess) oxygen coverage favors coupling. The results observed here suggest that higher selectivities and conversions should be obtainable under steady state catalytic conditions than heretofore observed [3, 6]. We are currently investigating this matter further.

The work herein provides insight into the ongoing discussion regarding the roles of Ag and Au in determining the chemical behavior of npAu. Key to the mechanism for coupling is β-hydride elimination from adsorbed alkoxy to form the aldehyde, which then reacts with another adsorbed alkoxy to yield the ester. The temperature at which β-C–H bond scission occurs must therefore be less than or equal to the temperature at which the ester is evolved. The temperatures for β-C–H bond scission for ethoxy on npAu, Ag(110), Au(111) and methoxy on a model $Ag_{0.4}/Au_{0.6}(111)$ alloy surface [15] are all slightly different (Table 1). What is most striking about this comparison is that the temperature for activation of the C–H bond on npAu is significantly higher than that of both the model Au(111) surface and the Ag/Au alloy surface and is close to the temperature observed on metallic silver. This comparison suggests that activation of the alkoxy species occurs on sites involving Ag.

Our investigation also establishes that coarsening of npAu does not eliminate its activity for selective oxidation of ethanol, including self-coupling to ethyl acetate. Although repeated thermal cycling during cleaning and temperature programmed reaction studies changes the ligament structure (Fig. 5), the overall pattern of reactivity remains consistent. The changes in selectivity are attributed to a different catalyst surface composition and structure as the catalyst surface is dynamic and changes with high temperature and exposure to organic reagents [23, 30, 31]. The persistence of activity for ethanol coupling by coarsened npAu is in contrast to the absence of activity reported for CO oxidation on similarly coarsened material [32]. We attribute this difference in part to the fact that there are fewer low coordination sites on coarsened npAu. The binding of CO to Au and Ag is extremely weak in general; however, the binding is somewhat stronger on under coordinated atoms, as established for Au, for example [33, 34]. The weak binding of CO would result in a shorter surface lifetime on coarsened npAu and, therefore, a reduced reaction rate. The persistence of activity for ethanol coupling on the coarsened material indicates that the activation of O_2 on npAu is not strongly dependent on the ligament size and further suggests that the binding energy of ethanol is not strongly dependent on the presence of under coordinated metal atoms.

5 Conclusions

Oxygen-assisted self-coupling of ethanol and 1-butanol on npAu ingots readily occurs under the controlled conditions afforded by ultrahigh vacuum, reflecting the reaction mechanism observed previously on single crystal gold surfaces. The selectivity for the esters is characteristic of reactions on gold, whereas the oxygen dissociation is more characteristic of metallic silver. The npAu therefore appears to function as a bifunctional catalytic material, including, to a limited extent, competitive reactions on both the silver and gold at the surface. The facile self-coupling of ethanol and 1-butanol observed here indicates that their self-coupling should occur readily over npAu in a flow reactor under appropriate conditions.

Acknowledgments We gratefully acknowledge the support of this work by the U.S. Department of Energy, Basic Energy Sciences, Catalysis Science Program (DE-FG-02-84ER13289). Work at LLNL was performed under the auspices of the U.S. Department of Energy by LLNL under Contract DE-AC52-07NA27344. Correspondence and requests for materials should be addressed to C.M.F.

References

1. Pina Della C, Falletta E, Prati L, Rossi M (2008) Selective oxidation using gold. Chem Soc Rev 37:2077
2. Stratakis M, García H (2012) Catalysis by supported gold nanoparticles: beyond aerobic oxidative processes. Chem Rev 112:4469
3. Pina CD, Falletta E, Rossi M (2011) Update on selective oxidation using gold. Chem Soc Rev 41:350
4. Kosuda KM, Wittstock A, Friend CM, Bäumer M (2012) Oxygen-mediated coupling of alcohols over nanoporous gold catalysts at ambient pressures. Angew Chem Int Ed 51:1698
5. Liu X, Xu B, Haubrich J et al (2009) Surface-mediated self-coupling of ethanol on gold. J Am Chem Soc 131:5757
6. Wittstock A, Zielasek V, Biener J et al (2010) Nanoporous gold catalysts for selective gas-phase oxidative coupling of methanol at low temperature. Science 327:319

7. Wang L-C, Stowers KJ, Zugic B et al (2015) Methyl ester synthesis catalyzed by nanoporous gold: from 10–9 Torr to 1 atm. Catal Sci Technol 5:1299
8. Stowers KJ, Madix RJ, Friend CM (2013) From model studies on Au(111) to working conditions with unsupported nanoporous gold catalysts: oxygen-assisted coupling reactions. J Catal 308:131
9. Xu B, Madix RJ, Friend CM (2010) Achieving optimum selectivity in oxygen assisted alcohol cross-coupling on gold. J Am Chem Soc 132:16571
10. Xu B, Liu X, Haubrich J et al (2009) Selectivity control in gold-mediated esterification of methanol. Angew Chem Int Ed 48:4206
11. McCarty J, Falconer JL, Madix RJ (1973) Decomposition of formic acid on Ni(110) I. Flash decomposition from the clean surface and flash desorption of reaction products. J Catal 30:235
12. Xu B, Madix RJ, Friend CM (2012) Dual-function of alcohols in gold-mediated selective coupling of amines and alcohols. Chem Lett 18:2313
13. Campbell CT (1985) Atomic and molecular oxygen adsorption on Ag(111). Surf Sci 157:43
14. Barteau MA, Madix RJ (1980) The adsorption of molecular oxygen species on Ag(110). Surf Sci 97:101
15. Xu B, Siler CGF, Madix RJ, Friend CM (2014) Ag/Au mixed sites promote oxidative coupling of methanol on the alloy surface. Chemistry 20:4646
16. Cremer T, Siler CGF, Rodríguez-Reyes JCF et al (2014) Tuning the stability of surface intermediates using adsorbed oxygen: acetate on Au(111). J Phys Chem Lett 5:1126
17. Gong J, Mullins CB (2008) Selective oxidation of ethanol to acetaldehyde on gold. J Am Chem Soc 130:16458
18. Xu B, Madix RJ, Friend CM (2014) Predicting gold-mediated catalytic oxidative-coupling reactions from single crystal studies. Acc Chem Res 47:761
19. Erlebacher JJ, Aziz MJM, Karma AA et al (2001) Evolution of nanoporosity in dealloying. Nature 410:450
20. Zugic B, Madix RJ, Friend CM, forthcoming
21. Tan YH, Davis JA, Fujikawa K et al (2012) Surface area and pore size characteristics of nanoporous gold subjected to thermal, mechanical, or surface modification studied using gas adsorption isotherms, cyclic voltammetry, thermogravimetric analysis, and scanning electron microscopy. J Mater Chem 22:6733
22. Fajín JLC, Cordeiro MNDS, Gomes JRB (2011) On the theoretical understanding of the unexpected O_2 activation by nanoporous gold. Chem Commun 47:8403
23. Moskaleva LV, Röhe S, Wittstock A et al (2011) Silver residues as a possible key to a remarkable oxidative catalytic activity of nanoporous gold. Phys Chem Chem Phys 13:4529
24. Czanderna AW (1964) The Adsorption of oxygen on silver. J Phys Chem 68:2765
25. Canning N, Outka D, Madix RJ (1984) The adsorption of oxygen on gold. Surf Sci 141:240
26. Backx C, De Groot C, Biloen P (1981) Adsorption of oxygen on Ag (110) studied by high resolution ELS and TPD. Surf Sci 104:300
27. Campbell CT (1986) An XPS study of molecularly chemisorbed oxygen on Ag(111). Surf Sci 173:L641
28. Gottfried JM, Schmidt KJ, Schroeder S, Christmann K (2003) Oxygen chemisorption on Au (110)-(1 × 2) II. Spectroscopic and reactive thermal desorption measurements. Surf Sci 525:197
29. Eric Klobas J, Schmid M, Friend CM, Madix RJ (2014) The dissociation-induced displacement of chemisorbed O_2 by mobile O atoms and the autocatalytic recombination of O due to chain fragmentation on Ag(110). Surf Sci 630:187
30. Kralik M, Macho V, Jurecekova E (1998) The oxidative dehydrogenation of alkanes C-3-C-4 by carbon dioxide. Chem Pap 52:682
31. Bharadwaj SS, Yokoyama C, Schmidt LD (1996) Catalytic partial oxidation of alkanes on silver in fluidized bed and monolith reactors. Appl Catal A 140:73
32. Wittstock A, Bäumer M (2013) Catalysis by unsupported skeletal gold catalysts. Acc Chem Res 47:731
33. Risse T, Shaikhutdinov S, Nilius N et al (2008) Gold supported on thin oxide films: from single atoms to nanoparticles. Acc Chem Res 41:949
34. Starr DE, Shaikhutdinov SK, Freund HJ (2005) Gold supported on oxide surfaces: environmental effects as studied by STM. Top Catal 36:33